MECSOL 2022 - Proceedings of the 8th International Symposium on Solid Mechanics
M.L. Bittencourt, J. Labaki, L.C.M. Vieira Jr. and E. Mesquita (Editors), Campinas SP, Brazil, October 17th to 19th, 2022

# Effect of physical and optimization parameters on the topology optimization of foundations and buried structures

**Aldemar Siqueira[1], Renato Picelli[2] and Josué Labaki[1]**

[1] School of Mechanical Engineering, University of Campinas, 200 Mendeleyev St, 13083-860, Campinas SP, Brazil
[2] Department of Mining and Petroleum Engineering, University of São Paulo, Praça Narciso de Andrade s/n, Vila Mathias, Santos - SP, 11013-560, Brazil

*Abstract. The topology optimization of the multiphysics problem of soil-structure interaction has a few significant differences from that of classical problems involving bounded, homogeneous domains. Among the most outstanding differences, is that the continuous soil-structure contact interface and the behavior of the soil as an unbounded, flexible medium have a significant impact on the evolution of the iterative optimization procedure and in the resulting optimal topologies. Differently than in bounded-domain problems, evolving topologies of buried structures present varying values of stiffness arising from their contact with the soil, in addition to the stiffness corresponding to the topology of the structure itself. This composition of phenomena causes the optimization algorithm to be significantly more strongly affected by physical and optimization parameters than in classical bounded-domain problems. In this paper, we study the effect of selected parameters in the topology optimization of foundations and buried structures. For this analysis, we use a coupled boundary-finite element model of buried structures, which accurately accounts for the response of the soil as an unbounded medium. The classical Bi-directional Evolutionary Structure Optimization (BESO) method is used to minimize the compliance of the buried structure under prescribed volume restriction. The paper discusses how the size and shape of the initial design volume and soil flexibility affect the optimization process. Under controlled conditions, similarly well-performing local minima can be found, although corresponding to starkly different optimal topologies.*
***Keywords: topology optimization, BESO, soil-structure interaction, coupled methods***

## INTRODUCTION

Nowadays, there are different well-established topology optimization algorithms that have been applied to the most diverse practical problems of engineering, ranging from multiphysics systems (Picelli *et al*, 2020) to multiscale multiphase structures (Gao *et al*, 2019). On the other hand, problems with unbounded domains, for example soil-structure interaction problems, have not been studied as deeply as bounded domain problems. More specifically, there are only a few works in the literature regarding the optimization of geotechnical structures.

In recent years, the first significant study concerning a geotechnical problem is due to Pucker and Grabe (2011), which considered a two-dimensional model of the soil and applied the Solid Isotropic Material with Penalization (SIMP) method to optimize the foundation topology of a rigid footing. They observed that the optimized topology is equivalent to a couple of piles connected to the edges of footing. This work was extended by Seitz and Grabe (2016) by considering a 3D analysis, which obtained similar results. Both these works used finite elements to discretize a large, adequately constrained domain representing the soil. Although they have relatively low computational cost, the finite element discretizations are not capable of accurately represent the stress distributions in the soil. Recently, Cavalcante *et al* (2022) studied topology optimization of 3D piled-structures and Cortez *et al* (2022) investigated the influence of soil flexibility on the topology optimization of a structure with continuous contact with soil. These works used boundary element formulations to accurately model the soil response and their results show that optimized topologies for structures interacting with the soil are strongly dependent on the soil flexibility.

In this work, classical BESO algorithm is used to optimize the topology of a partially buried structure. The embedded structure and a portion of soil are modeled via the Finite Element Method (FEM), and an Indirect Boundary Element Method (IBEM) formulation is used to accurately model the unbounded behavior of soil, which is considered as a semi-infinite elastic medium. An IBEM-FEM coupling scheme is derived. The optimized topologies for the buried foundation of a rigid strip footing are presented. The influence of structure's initial design and IBEM-FEM interface on the optimization results is investigated.

## NUMERICAL MODEL

### Problem statement

Consider a two-dimensional, linear-elastic, arbitrarily-shaped structure of Young's modulus $E_c$ and Poisson ratio $\nu_c$ partially buried in a horizontally-unbounded linear-elastic layer of Young's modulus $E_s$, $\nu_s$, and depth $H$, resting over a rigid bedrock (Fig. 1a). The optimization problem can stated as: given a prescribed volume of material, what is the optimal topology for the buried portion of the structure that results in the stiffest soil-structure system.

### Soil-structure interaction model

In this work, the soil-structure interaction is modeled by a boundary-finite element coupling scheme. In this scheme, a rectangularly-shaped domain $\Omega$, comprising the embedded part of the structure is modeled with classical four-noded finite elements (Fig. 1b), so that any finite element in $\Omega$ may assume the material properties of the structure, denoted by the sub-index $c$, those of the surrounding soil, denoted by the sub-index $s$, or represent voids in the structure. The rest of the semi-infinite soil layer is modeled via an Indirect Boundary Element Method formulation, in which thse interface $\Gamma = \Gamma_1 + \Gamma_2 + \Gamma_3$ (Fig. 1c) is discretized with piece-wise constant boundary elements representing a superposition of non-singular influence functions.

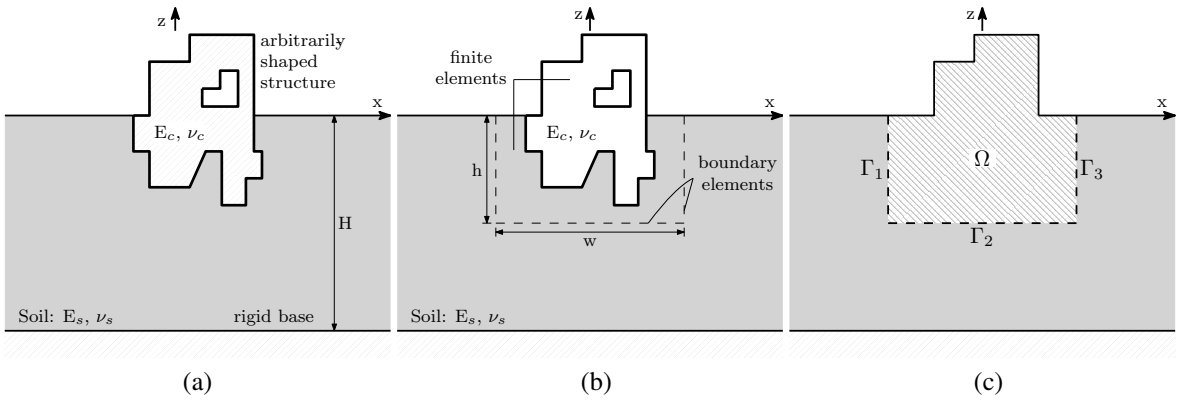


**Figure 1 – a) arbitrarily-shaped structure buried in the soil, b) subdomains used in the finite- and boundary-element models, and c) subdomain notation.**

### Model of the Structure

The domain $\Omega$ is modeled with linear-elastic, plane-strain, isoparametric quadrilateral finite elements (FE), with four nodes and two degrees of freedom (horizontal and vertical displacements) per node. The elemental stiffness matrix is given by: $\mathbf{k}_c = \int_{-1}^{+1}\int_{-1}^{+1} \mathbf{B}^T\mathbf{C}\mathbf{B}\det[\mathbf{J}]d\xi d\eta$, where $\mathbf{B}$ is the strain-displacement transformation matrix, $\mathbf{C}$ is the constitutive matrix for the plane strain case and $\mathbf{J}$ is the Jacobian operator of the transformation between natural $(x-z)$ and parametric $(\xi-\eta)$ domains. The global stiffness matrix $\mathbf{K}_c$ of $\Omega$ is assembled from $\mathbf{k}_c$ according to the classical assembly algorithm (Bathe, 2006), and the equilibrium equation of $\Omega$ is given by

$$\mathbf{K}_c\mathbf{u}_c = \mathbf{f}_c, \tag{1}$$

in which $\mathbf{u}_c$ and $\mathbf{f}_c$ are the vector of nodal displacements and forces, respectively.

### Model of the soil layer

The IBEM formulation used to model the soil layer consists in connecting displacements and tractions at discrete points in the medium through a set of fictitious loads. In the present model, the interface $\Gamma$ is discretized by $N_s = N_h + 2N_w$ piece-wise constant boundary elements (BE), in which $N_w$ is the number of vertical elements at $\Gamma_1$ and $\Gamma_3$, and $N_h$ is the number of horizontal elements at $\Gamma_2$. Each element has a central node where displacements and tractions are measured, which can be written as

$$\mathbf{u}_b = \mathbf{U}\mathbf{q}, \tag{2}$$

$$\mathbf{t}_b = \mathbf{T}\mathbf{q}, \tag{3}$$

in which $\mathbf{u}_b = \left\{u_x^1\ u_z^1\ u_x^2\ u_z^2 \ldots u_x^{N_s}\ u_z^{Ns}\right\}^T$ is the vector of nodal displacements, $\mathbf{t}_b = \left\{t_x^1\ t_z^1\ t_x^2\ t_z^2\ \ldots t_x^{N_s}\ t_z^{Ns}\right\}^T$ is the vector of nodal tractions, $\mathbf{q} = \left\{q_x^1\ q_z^1\ q_x^2\ q_z^2 \ldots q_x^{N_s}\right\}^T$ is the vector of fictitious loads, and $\mathbf{U}$ and $\mathbf{T}$ are displacement and traction influence matrices comprising the response of the soil layer. Sub and super indices of a general term $u_{r,s}^{i,j}$ of matrix $\mathbf{U}$ represent the displacement of an element $i$ of the BE mesh in the $r$-direction due to a unit load uniformly distributed over an element $j$ in the $s-$ direction $(i,\ j = 1,\ldots,N_s;\ r,s = x,z)$. The same convention holds for a general term $t_{r,s}^{i,j}$ of matrix $\mathbf{T}$. Prescribed continuity and equilibrium conditions given at the element nodes throughout $\Gamma$ must be satisfied in order to obtain the vector of unknown contact forces $\mathbf{q}$.

*Influence Functions*

The response of the semi-infinite soil layer is computed through solutions for stress and displacement fields due to non-singular loads applied to the soil. These solutions are called influence functions. In the present work, displacement and stress influence functions for buried loads are used. These solutions were recently presented by Cortez *et al.* (2022), and are written in terms of improper integrals in the Fourier transformed space:

$$u_i(x,z) = \int_{-\infty}^{\infty} \bar{u}_i\, e^{i\zeta x} d\zeta, \tag{4}$$

$$\sigma_{ij}(x,z) = \int_{-\infty}^{\infty} \bar{\sigma}_{ij}\, e^{i\zeta x} d\zeta, \quad i,j = x,z, \tag{5}$$

where $\bar{u}_i$ and $\bar{\sigma}_i$ are functions of the elastic constants and load depth. These integrals are evaluated numerically, which is the most time-consuming task in the present formulation because their integrand contains singularities, and an oscillatory-decaying tail, making the use of classical quadrature integration schemes inadequate for this task. Further discussion and details on the numerical evaluation of these integrals can be found in Cortez *et al.*, 2022.

The terms of the traction influence matrix (Eq. (3)) are given in terms of stress influence functions by the Cauchy's formula $t_{rt}^{i,j} = \sigma_{rst}^{i,j} n_r^i$, $(r,s,t = x,z;\ i,j = 1,\ldots,N_s)$, in which $\mathbf{n}^i = \left\{n_x^i\ n_z^i\right\}^T$ is the unit normal vector at the BE where the traction is being measured, pointing outward the soil domain. At $\Gamma_1$, $\Gamma_2$ and $\Gamma_3$, $\mathbf{n}^i = \{1\ 0\}^T$, $\mathbf{n}^i = \{0\ 1\}^T$, $\mathbf{n}^i = \{-1\ 0\}^T$, respectively. Influence functions for loads that are uniformly distributed in the vertical direction are used for elements placed at $\Gamma_{1,3}$ while influence functions for loads that are uniformly distributed in the horizontal direction are used for elements at $\Gamma_2$.

## Structure-soil coupling

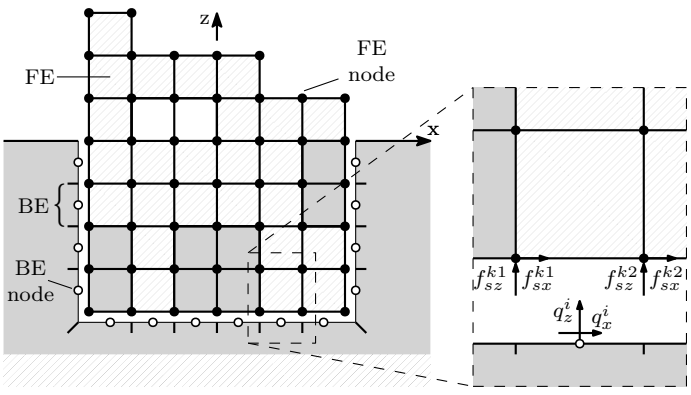


**Figure 2 – Coupling.**

The present model considers a one-to-one finite-boundary element correspondence discretization of $\Omega$ and $\Gamma$. The soil response over $\Omega$ is incorporated through a set of equivalent nodal contact forces $\mathbf{f}_s$, acting on finite element nodes at $\Gamma$. Therefore, the equilibrium equation of $\Omega$ (Eq. (1)) becomes

$$\mathbf{K}_c\mathbf{u}_c = \mathbf{f}_c - \mathbf{f}_s. \tag{6}$$

Coupling between $\Omega$ and the surrounding soil consists of imposing equilibrium and continuity conditions at the $\Gamma$ interface. The equilibrium condition represents a force equilibrium between the contact forces acting on a boundary element, written in terms of $\mathbf{q}$, and the nodal forces of its corresponding finite element, written in terms of $\mathbf{f}_s$. Considering that each BE is connected to a couple of FE nodes (see Fig. 2), a nodal equivalency transformation given by $\mathbf{f}_s = \mathbf{A}\mathbf{q}$ can be used to represent the equilibrium. In this equation, $\mathbf{f}_s = \left\{ f_{sx}^1 \; f_{sz}^1 \; f_{sx}^2 \; f_{sz}^2 \ldots f_{sx}^{n_n} \; f_{sz}^{n_n} \right\}$ and $\mathbf{A}$ is a transformation matrix.

In view of this transformation, Eq. (6) can be rewritten as

$$\mathbf{K}_c\mathbf{u}_c + \mathbf{A}\mathbf{T}\mathbf{q} = \mathbf{f}_c. \tag{7}$$

The continuity condition imposes that the displacement at each BE is consistent with the nodal displacements of its corresponding FE. This can also be written in terms of a linear transformation given by:

$$\mathbf{u}_b = \mathbf{D}\mathbf{u}_c, \tag{8}$$

in which $\mathbf{D}$ is a transformation matrix. A full description of the transformation matrices $A$ and $D$ can be found in Cortez *et al.* (2022).

In view of Eq. (2) this continuity condition yields

$$\mathbf{D}\mathbf{u}_c - \mathbf{U}\mathbf{q} = \mathbf{0}. \tag{9}$$

Equations (8) and (11) can be written as a single matrix equation,

$$\begin{bmatrix} \mathbf{K} & \mathbf{A}\mathbf{T} \\ \mathbf{D} & -\mathbf{U} \end{bmatrix} \begin{Bmatrix} \mathbf{u}_c \\ \mathbf{q} \end{Bmatrix} = \begin{Bmatrix} \mathbf{f} \\ \mathbf{0} \end{Bmatrix}, \tag{10}$$

which represents the equilibrium equation for nodes at the interface $\Gamma$, and

$$\begin{bmatrix} \mathbf{K} & \begin{Bmatrix} \mathbf{A}\mathbf{T} \\ \mathbf{0} \end{Bmatrix} \\ \begin{Bmatrix} \mathbf{D} & \mathbf{0} \end{Bmatrix} & -\mathbf{U} \end{bmatrix} \begin{Bmatrix} \begin{Bmatrix} \mathbf{u}_c \\ \mathbf{0} \end{Bmatrix} \\ \mathbf{q} \end{Bmatrix} = \begin{Bmatrix} \begin{Bmatrix} \mathbf{f} \\ \mathbf{0} \end{Bmatrix} \\ \mathbf{0} \end{Bmatrix}, \tag{11}$$

in which $\mathbf{0}$ are matrices of zeros of compatible dimensions. The solution of Eq. (11) for a set of prescribed contact forces $\mathbf{f}$ yields the nodal displacements $\mathbf{u}_c$ of $\Omega$, as well as the set of fictitious loads $\mathbf{q}$, with which displacement and stress solutions can be computed anywhere in the soil domain.

## TOPOLOGY OPTIMIZATION

In general, the optimizable domain $\Omega$ is composed by two subdomains: one buried in the soil, comprising the embedded part of the structure, and another outside the soil composed only by the structure. In this article, only the buried subdomain is considered, resulting in a foundation topology optimization problem. The optimal foundation must have the largest possible stiffness for a prescribed volume of material. This characterizes a compliance minimization problem subjected to a volume constraint. In the sense of the present coupled IBEM-FEM formulation, this problem can be formulated as

$$\begin{aligned} &\underset{x_i}{\text{Minimize:}}\; C(x_i) = \mathbf{f}^T\mathbf{u}_d, \\ &\text{Subject to:}\; V_r \leq \bar{V}_r, \\ &\qquad\qquad \mathbf{K}\mathbf{u}_d = \mathbf{f}, \\ &\qquad\qquad x_i \in \{0,1\},\; i \in [1,N_d], \end{aligned} \tag{12}$$

in which $x_i$ is the vector of design variables, $\bar{V}_r$ is the specified maximum of structure material, $N_d$ is the number of elements in the design domain, and $C(x)$ is the structural compliance, the objective function. The design variables represent the physical density of an element with $x_i = 1$ corresponding to a structure element and $x_i = 0$ to a soil element. No intermediate values are considered given that BESO is a binary variables algorithm.

### Material interpolation scheme

As elements in $\Omega$ can assume properties of the structure or the soil, a two-phase material interpolation scheme is used (Bendsøe and Sigmund, 1999):

$$E(x_i) = E_s + x_i^p (E_c - E_s). \tag{13}$$

### Sensitivity numbers

Sensitivity numbers represent the gradient of the objective function with respect to individual element density. The influence matrices, $U$ and $T$, and coupling matrices, $D$ and $A$, are not dependent on the elastic properties of the optimizable domain $\Omega$. Therefore, the elemental sensitivities depende only on the coupled structural stiffness and not on the properties of the unbounded layer. Consequently, elemental sensitivities can be written as (Huang and Xie, 2009)

$$\alpha_i = \begin{cases} \left[1 - \dfrac{E_s}{E_c}\right] \mathbf{u}_i{}^T \mathbf{k}_i \mathbf{u}_i, & \text{for structure element} \\ 0, & \text{for soil element,} \end{cases} \tag{14}$$

where $\mathbf{k}_i$ and $\mathbf{u}_i$ are the elemental stiffness matrix and the vector of nodal displacements of element $i$, respectively. The sensitivity numbers in Eq. (14) are obtained when the penalty factor in Eq. (13) tends to infinity, characterizing a hard-kill approach, which was chosen for this implementation for its lower computational cost in comparison to the soft-kill approach while giving similar results.

### BESO algorithm

The classical Bi-directional Evolutionary Structural Optimization method (BESO) is an iterative algorithm presented by Huang and Xie (2007) that optimizes material distribution in design domain based on a rank of elemental sensitivity numbers (Eq. (14)). At each iteration, sensitivity numbers are computed based on the results of a finite element analysis; then, elements are simultaneously added and removed from the domain, seeking the stiffest material distribution until the volume constraint and a convergence criterion are satisfied. The net amount of material added or removed at each iteration is controlled by an evolutionary ratio ($ER$), given as a percentage of the design domain volume. The total number of added elements is limited by a maximum admission ratio ($AR_{max}$), also given as a percentage of the design domain volume.

A smoothing filter is applied to the sensitivity numbers to avoid numerical instabilities such as checkerboard patterns and mesh-dependency. In this work, the filtered sensitivity number $\hat{\alpha}_i$ of element $i$ is given by

$$\hat{\alpha}_i = \frac{\sum_{j=1}^{N_d} \alpha_i H_{ij}}{\sum_{j=1}^{N_d} H_{ij}}, \tag{15}$$

where $H_{ij} = \max\{0, r_f - r_{ij}\}$, $r_f$ is the filter radius and $r_{ij}$ is the distance between the centers of the $i$-th and $j$-th elements.

The sensitivity numbers of consecutive iterations are averaged in order to enhance optimization convergence properties as proposed by Huang and Xie (2007). This is obtained by

$$\hat{\alpha}_i^k = \frac{\hat{\alpha}_i^k + \hat{\alpha}_i^{k-1}}{2}, \tag{16}$$

where $k$ denotes the current iteration.

The following convergence criterion is used

$$\text{error} = \frac{\left|\sum_{i=1}^{N}\left(C_{k-i+1} - C_{k-N-i+1}\right)\right|}{\sum_{i=1}^{N} C_{k-i+1}} \leq \tau, \tag{17}$$

where $k$ is the current iteration number, $\tau$ is an allowable convergence error and $N$ is a prescribed arbitrary integer. All examples presented in this paper consider $\tau = 10^{-4}$ and $N = 5$. This means that the compliance must be stable for at least ten consecutive iterations in order to satisfy convergence.

## NUMERICAL RESULTS

In this section, the application of the present formulation is illustrated by considering the problem of a vertically loaded rigid strip footing laying on the soil surface. A footing of width $a$, under centered and excentric vertical loads is considered. Given the unbounded nature of the soil-structure interaction problem, the choice of the size of the optimizable region is arbitrary. Based on Seitz and Grabe (2016), a square design domain, with $w = 4a$ and $h = 4a$, is considered (domain $A$) presented in Fig. 3. The plate and design domain are discretized with a homogeneous mesh of four-noded finite elements with element size of $0.04a$ (total of $1\times10^4$ elements). All results consider $E_c = 100E_s$, $\nu_c = \nu_s = 0.25$ and $H = 40$, which are practical engineering values. The BESO parameters used are $ER = 1\%$ , $AR_{\max} = 1\%$ and filter radius of 2.5 times the element size. The influence of the initial foundation design and the domain boundary on the final topology are investigated.

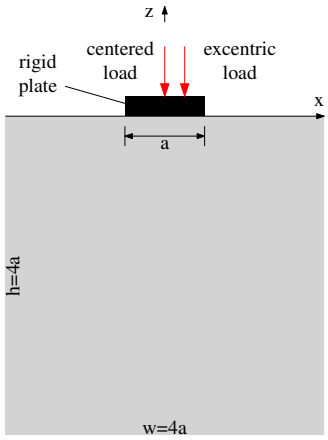


**Figure 3 – Domain $A$.**

### Full design

Figure 4 presents the final buried foundation topologies and the evolution of the structural compliance obtained for the centered and excentric load cases. These examples consider BESO starting from the full design (design domain is initially filled only with structure elements) and that the volume of available material for the structure is $vf = 5\%$ of the volume of the design domain. For the centered load case, the buried foundation is formed at both edges of the plate, symmetrically forming inclined pile-like structures, while, for the excentric load case, the foundation is concentrated almost exclusively at the most loaded edge, also in an inclined pile-like geometry. These results agree with Pucker and Grabe (2011) and Seitz and Grabe (2016).

Quantitative results for evolution the evolution of the compliance through iterations of optimization algorithm are presented in Fig. 4 in two curves: first, the total structural compliance of the buried domain, here named as $C_d$ (circle), which is the one considered in the convergence criterion given by Eq. (18); and second, the portion of compliance due only to foundation elements, here named as $C_f$ (triangle). In both loading cases, note that $C_d$ increases monotonically as the algorithm removes elements of the structure, on the other hand, $C_f$ reaches a peek and eventually decreases until convergence. To illustrate this evolution, Fig. 5 shows the topologies at four different stages of the optimization for the centered load case. Initially, foundation material is removed at lateral regions and at the center of domain (Fig. 5a). At iteration 100 (Fig. 5b), the foundation appears as a truss-like structure, connecting the footing to the bottom of domain. Two prominent bars can be observed among some thin connecting elements. After 100 more iterations (Fig. 5c), only

the two piles are present, still connecting the footing to the bottom of the domain. From this point on, these piles are disconnected from the bottom and begin to shorten. Lastly, at iteration 240 (Fig. 5d), the two piles are already detached from the bottom and continue to shorten until final topology in Fig. 4. Note that topology is such that the material is distributed so that the foundation reaches to deepest possible point in the soil with the material that is available, which is physically consistent with engineering practice.

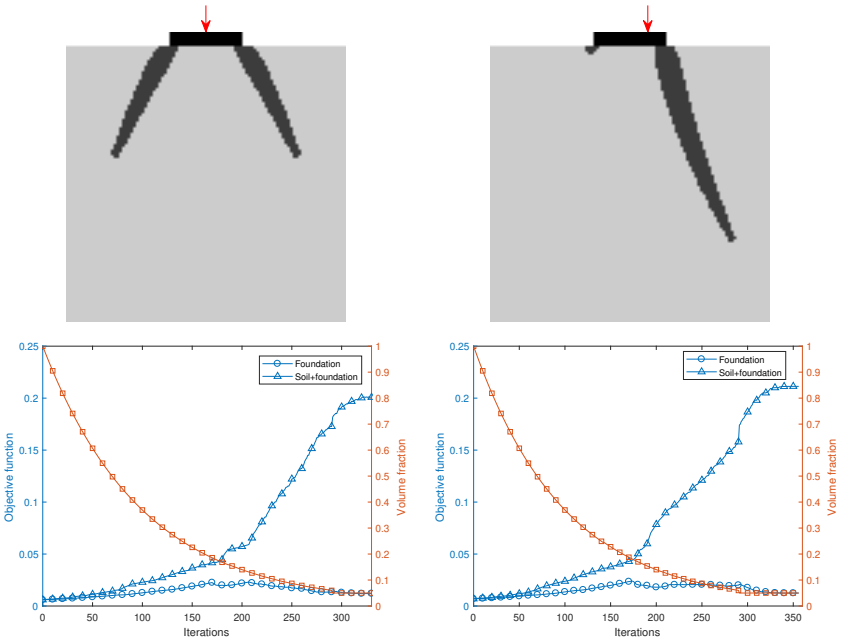


**Figure 4 – The final foundation topologies and evolution of objective function for the centered and excentric load cases.**


**Figure 5 – Evolution of foundation topology: (a) iteration 5, (b) iteration 100, (c) iteration 200 and (d) iteration 240.**

## Influence of initial design

In addition to the optimization results starting from the full design, Figure 6 illustrates the influence of the initial structure design on the optimization results for centered loaded footing with $v_f = 5\%$. Three different initial designs are considered: I, II and III with the volume of the structure corresponding to 25%, 50% and 75% of the volume of the design domain, respectively. The final foundations obtained from initial designs I and II have the same topologies, corresponding to a truss, while the final topology obtained from initial design III is the same pile-like foundation on obtained from the full design. Note that the truss foundation results in a less stiff soil-structure system than the pile foundation, characterizing a local minimum solution of the optimization problem. These results indicate that the optimized topology obtained by the classical BESO algorithm for this problem is dependent of the initial design. This is generally called the local minima problem and the classical BESO algorithm does not handle it well (Ghabraie, 2015). When the initial design is closer to

the soil surface (I and II), BESO material removal tend to generate unstable piles (short and/or very inclined) which end up converging to the truss-like foundation as illustrated for the initial design I in Fig. 7.

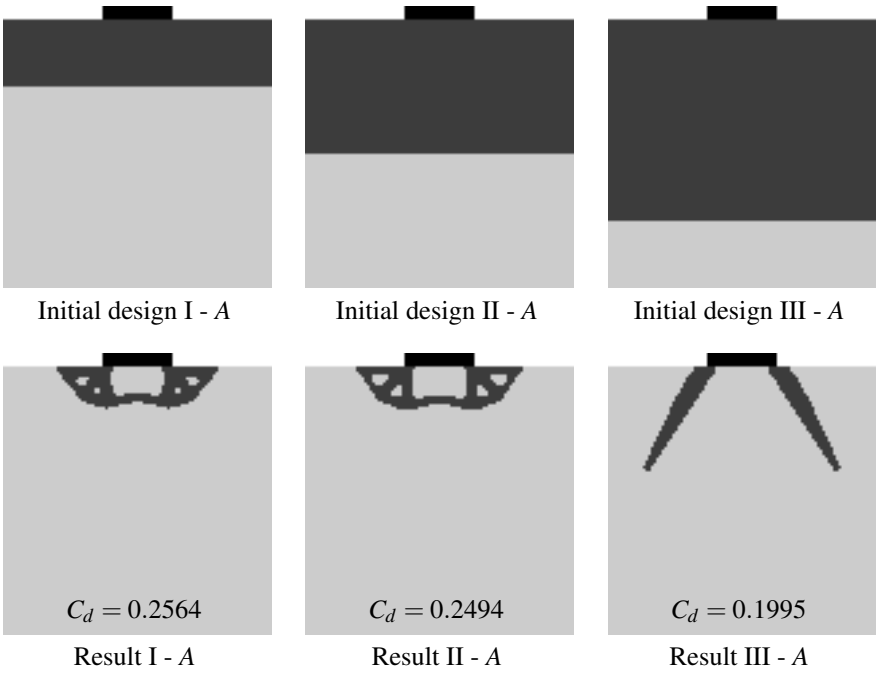


**Figure 6 – The final topologies for initial designs I, II and III on domain $A$.**

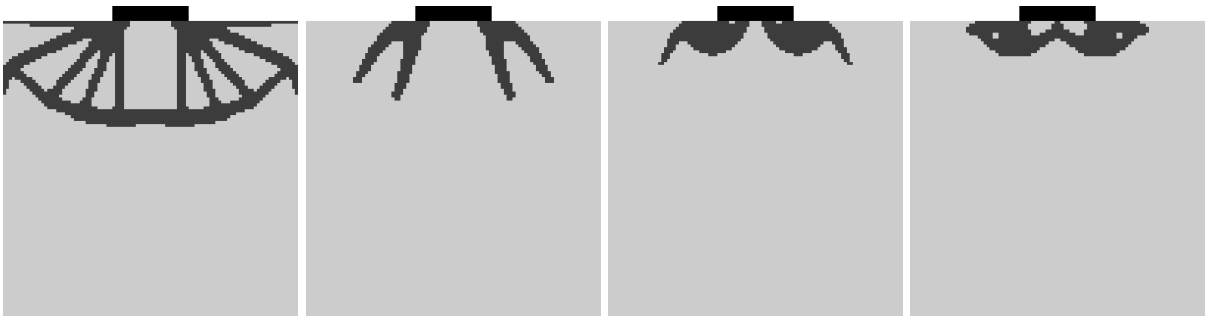


**Figure 7 – Evolution of foundation topology for the initial design I: (a) iteration 50, (b) iteration 160, (c) iteration 178 and (d) iteration 200.**

## Influence of domain boundary

In order to investigate the influence of the domain boundary on the optimization results, a larger design domain region (domain $B$), with $w = 8a$ and $h = 8a$, is considered. The same initial designs I, II and III shown in Fig. 6 are used in this analysis, which aims to determine if the BESO algorithm is able to reproduce the same final topologies shown in Fig. 6 without the initial soil-foundation interface being constrained by the FE-BE coupling interface. Note that, in this analysis, there are no interface loads directly applied to the nodes at the initial soil-foundation interface. The same amount of structure volume considered for domain $A$ is repeated here, representing $v_f = 1.25\%$ of the volume of domain $B$. Figure 9 shows the final optimization results obtained for domain $B$. Note the larger values of $C_d$ in comparison to the results for domain $A$, as domain $B$ comprises a larger region of the soil. The algorithm finds identical solutions for the initial designs I and III on domains $A$ and $B$, even reproducing the same local minimum. For the initial domain II, the final topologies obtained for domains $A$ and $B$ are similar but differ by the presence of a horizontal bar. Despite this difference, these

solutions have similar values of $C_d$, and represent similar local minima. By comparing the optimization results obtained from the domains $A$ and $B$, it is observed that the FE-BE interface has little influence on the final optimization results. This confirms the physical consistency of the present coupled formulation as the domain boundary does not represent a physical constraint, but only the response of the unbounded medium.

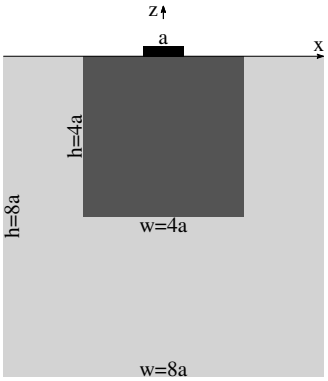


**Figure 8 – Domain $A$ modeled as an initial design in domain $B$.**

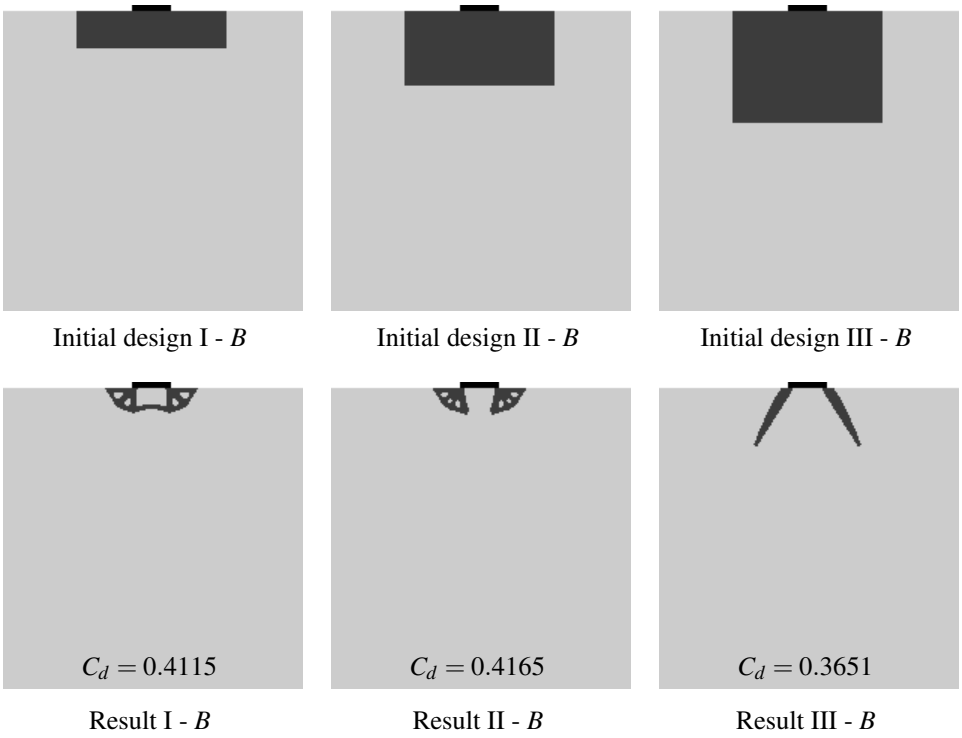


**Figure 9 – The final topologies for initial designs I, II and III modeled in domain $B$.**

## CONCLUSIONS

In this work, a coupled finite-boundary-element framework was used together with the classical BESO design algorithm to optimize the topology of a partially buried structure. The soil was modeled as a linear elastic, homogeneous, semi-infinite layer resting over a rigid bedrock. An Indirect-BEM formulation was used to compute the static response of the soil, represented by a set of equivalent nodal loads acting over an optimizable finite element domain. Results obtained for the optimized topology for the buried foundation of a rigid strip footing indicate that piled foundations have the largest

vertical stiffness, which is consistent with classical engineering results. The results also show that the present formulation is robust regarding the arbitrary definition of the optimizable design domain while it is sensitive to the initial structure designs.

## ACKNOWLEDGEMENTS

The authors acknowledge the financial support of Brazilian National Council for Scientific and Technological Development (CNPq) through grant 132194/2021-0 and São Paulo Research Foundation (Fapesp) through grant number 2018/05797-8 (Young Investigator Grant).

## REFERENCES

Picelli, R., Ranjbarzadeh, S., Sivapuram, R., Gioria, R.S. and Silva, E.C.N., 2020. "Topology optimization of binary structures under design-dependent fluid-structure interaction loads". *Structural and Multidisciplinary Optimization*, Vol. 62, No. 4, pp.2101-2116.

Gao, J., Luo, Z., Li, H. and Gao, L., 2019. "Topology optimization for multiscale design of porous composites with multi-domain microstructures." *Computer Methods in Applied Mechanics and Engineering*, Vol. 344, pp.451-476.

Pucker, T., and J. Grabe. "Structural optimization in geotechnical engineering: basics and application." *Acta Geotechnica 6*, Vol. 6, No. 1, pp. 41-49.

Seitz, K. F., Grabe, J., 2016. "Three-dimensional topology optimization for geotechnical foundations in granular soil". *Computers and Geotechnics, 80*, pp. 41-48.

Cavalcante I, Tavares E, Picelli R, Labaki J. "Influence of foundation flexibility on the topology optimization of piled structures." *International Journal for Numerical and Analytical Methods in Geomechanics*. 2022; (In Press).

Cortez, R., Sivapuram, R., Barros, P., Labaki, J. and Picelli, R., 2022. "On the influence of soil flexibility in structural topology". *Computer Methods in Applied Mechanics and Engineering*. Under Review.

Bathe. K.J., 2006. *Finite element procedures*. Klaus-Jurgen Bathe.

Bendsøe, M.P. and Sigmund, O., 1999. "Material interpolation schemes in topology optimization". *Archive of applied mechanics*, Vol. 69, No. 9, pp. 635-654.

Huang, X. and Xie, Y.M., 2009. "Bi-directional evolutionary topology optimization of continuum structures with one or multiple materials". *Computational Mechanics*, Vol. 43, No. 3, pp. 393–401.

Huang, X. and Xie, Y., 2007. "Convergent and mesh-independent solutions for the bi-directional evolutionary structural optimization method". *Finite elements in analysis and design*, Vol. 43, No. 14, pp. 1039–1049.

Ghabraie, K., 2015. "An improved soft-kill BESO algorithm for optimal distribution of single or multiple material phases". *Structural and multidisciplinary optimization*, Vol. 52, No. 4, pp. 773-790.

## RESPONSIBILITY NOTICE

The authors are the only parties responsible for the printed material included in this paper.